Journal of Orthopaedic Translation 52 (2025) 301–312

Contents lists available at ScienceDirect

Journal of Orthopaedic Translation

journal homepage: www.journals.elsevier.com/journal-of-orthopaedic-translation

Original article

Scleraxis-expressing progenitor cells are critical for the maturation of the annulus fibrosus and demonstrate therapeutic potential

Hongtao Jia [a], Shuqin Chen [b], Xuye Hu [c], Jiajun Wang [c], Jinlong Suo [d], Sheng-Ming Dai [a,*], Weiguo Zou [b,c,**], Heng Feng [c,***]

[a] *Department of Rheumatology & Immunology, Shanghai Sixth People's Hospital Affiliated to Shanghai Jiao Tong University School of Medicine, Shanghai, 200233, China*
[b] *Hainan Academy of Medical Sciences, Hainan Medical University, Haikou, 571199, China*
[c] *Key Laboratory of RNA Innovation, Science and Engineering, CAS Center for Excellence in Molecular Cell Science, Shanghai Institute of Biochemistry and Cell Biology, University of Chinese Academy of Sciences, Chinese Academy of Sciences, Shanghai, 200031, China*
[d] *Institute of Microsurgery on Extremities, and Department of Orthopedic Surgery, Shanghai Sixth People's Hospital Affiliated to Shanghai Jiao Tong University School of Medicine, Shanghai, 200233, China*

ARTICLE INFO

Keywords:
Annulus fibrosus (AF)
Scleraxis (*Scx*)
AF progenitor cells
Maturation and repair
Cell therapy

ABSTRACT

Background: Annulus fibrosus (AF) is an important part of the intervertebral disc (IVD) and its injury leads to back pain and impaired mobility. The stem/progenitor cells are essential for the maturation and repair of the AF, however, the identity of AF stem/progenitor cells remain elusive.
Methods: In this study, we sorted cells from the murine IVDs and performed the single-cell RNA sequencing. Using single-cell transcriptomics, genetic lineage tracing, *in vitro* stem cell experiment, ablation models and cell transplantation, we elucidate the role of AF progenitor cells in maturation and injury.
Results: On the basis of single-cell RNA-sequencing (scRNA-seq) analysis of the intervertebral disc, we found that the transcription factor *Scleraxis* (*Scx*) can specifically label a progenitor cell population of the outer AF. By lineage tracing assay, *Scx*-lineage AF cells proliferate mainly prior to sexual maturity, but barely proliferate after age of 8 weeks. The *Scx*-expressing AF cells are enriched for stem/progenitor cell markers and show a higher proliferative capacity and differentiation potential than the Scx^- cells. The ablation of *Scx*-expressing AF cells impairs the maturation of AF. The Scx^+ AF cells are enriched for TGFβ signaling. Transplantation of *Scx*-lineage cells to injured AF with Connective tissue growth factor (CTGF) improved the AF healing.
Conclusions: *Scleraxis*-expressing progenitor cells are critical for the maturation of AF and demonstrate therapeutic potential for AF regeneration.
The translational potential of this article: These findings expand the important role of stem cells in maturation and repair and provide new strategy for cellular therapy of AF repair.

1. Introduction

Lower back pain (LBP) causes maximum productivity loss worldwide and is the leading cause of years lived with disabilities [1]. The annual expenditures for the management of LBP patients are estimated to exceed $100 billion in the USA [2].

The intervertebral disc (IVD) connects the vertebraes and bears the pressure of the spine during movement. It consists of two important structures, the annulus fibrosus (AF) and the intermediate nucleus pulposus (NP). The AF is rich in collagen and made up of fibrocartilage, similar to the ligament structure. It surrounds the middle NP, a cartilage-like structure made up of proteoglycans [3]. AF can be divided into inner and outer regions. The outer AF is ligamentous tissue and the inner AF is cartilage-like tissue. The outer AF consists primarily of thick, dense type I collagen fibers, resulting in higher stiffness, while the inner AF contains thin, loose type II collagen fibers [4–6].

* Corresponding author.
** Corresponding author. Key Laboratory of RNA Innovation, Science and Engineering, CAS Center for Excellence in Molecular Cell Science, Shanghai Institute of Biochemistry and Cell Biology, University of Chinese Academy of Sciences, Chinese Academy of Sciences, Shanghai, 200031, China.
*** Corresponding author.
E-mail addresses: shengmingdai@163.com (S.-M. Dai), zouwg94@sibcb.ac.cn (W. Zou), fengheng2014@sibcb.ac.cn (H. Feng).

https://doi.org/10.1016/j.jot.2025.04.009
Received 13 November 2024; Received in revised form 15 April 2025; Accepted 16 April 2025

The AF cells are descendants of the *Scx*$^{+}$/Sox9^{+} progenitors [7]. Scleraxis (*Scx*) is important in tendon development, growth, and healing. *Scx*$^{+}$ cells are required for maintenance of collagen extracellular matrix (ECM) alignment and organization in adults, but not early post-natal flexor tendon growth [8]. *Scx* is the marker of tendon progenitor cells [9]. Previous studies found that *Scx* labels the caudal IVD cells of mice [10]. However, the characteristics of *Scx*-expressing progenitors and their therapeutic potential have not been explored.

Injuries of the AF result in the IVD herniation and degeneration. The main treatment is surgical removal of herniated tissue, but is difficult to repair AF, leading to recurrence. Relatively few studies have focused on the endogenous AF repair capacity [11]. Identifying unique biomarkers of the AF is essential to ensure the quality control measures of stem cells for regenerative treatments, which is an ongoing exploration [12]. AF-derived stem cells are multipotent and serve as ideal seed cells for AF repair due to their tissue-specific origin [13]. AF stem/progenitor cells express markers, including Col5a1, Col12a1, CD29, CD44, and CD166, and exhibit differentiation potential [14–16]. Although resident AF stem/progenitor cells have been identified in recent studies, there is still no consensus in the field on definitive markers for these cells or their location/potential [17].

In this study, we separated IVD cells from 8-week-old mice and performed single-cell RNA-Seq (scRNA-Seq). *Scx* was identified as a specific marker labeling outer AF cells. Lineage tracing revealed that

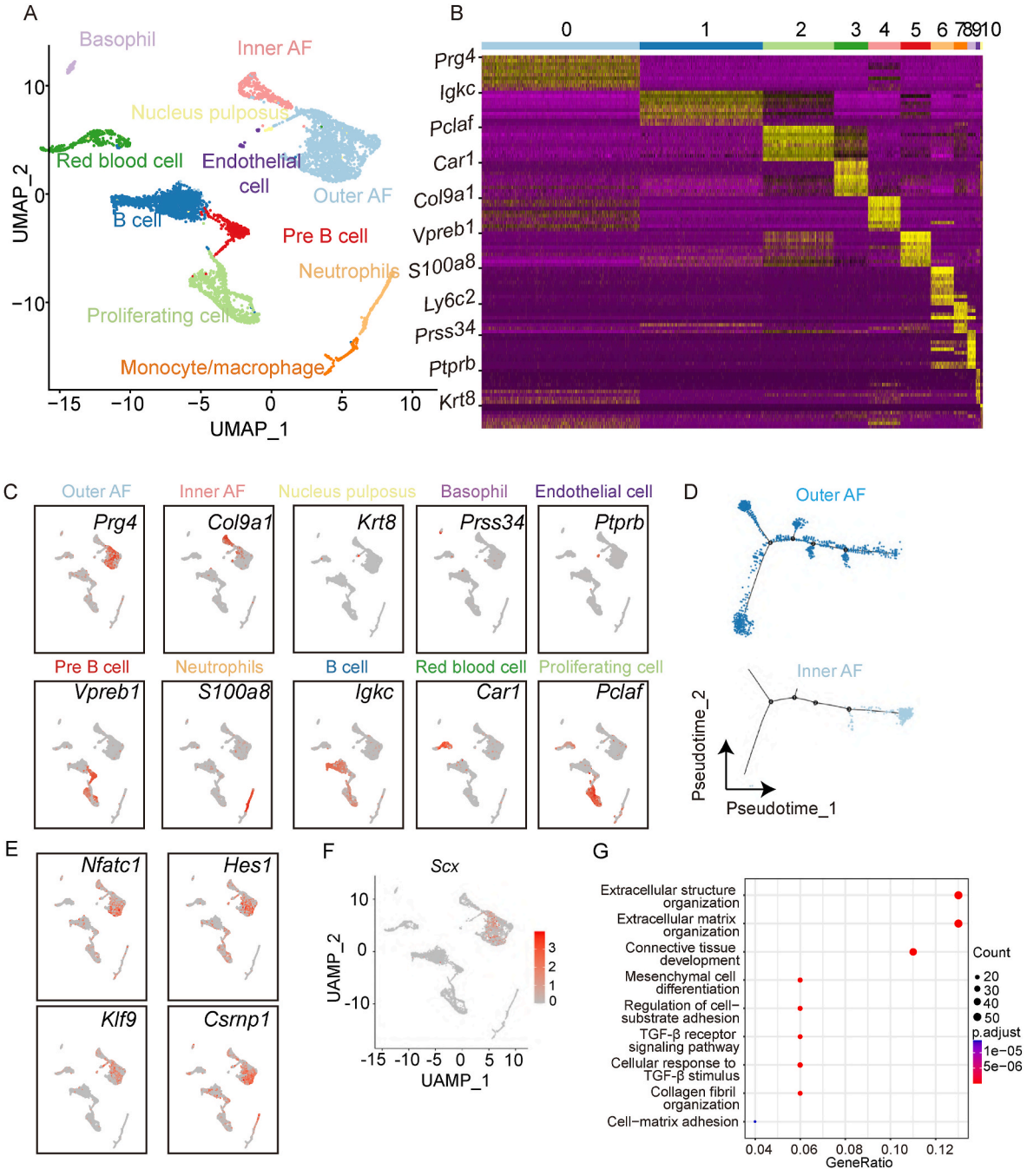

Fig. 1. Single-cell RNA sequencing analysis identified transcription factor Scx specifically labeled the cells of the outer annulus fibrosus
(A) UMAP grouping of the single cell RNA sequencing of intervertebral disc cells isolated from 8-week-old WT mice. (B) Heat map of gene expression in different cell groupings. (C) Marker gene expression in different groups. (D) Pseudotime analysis of cells from outer and inner AF. (E) Single cell data analysis of transcription factor expression in different groups. (F) Single cell data analysis of Scx expression in different groups. (G) GO analysis of *Scx*$^{+}$ AF cells.

Scx$^+$ AF cells contribute to AF maturation. *Scx*$^+$ AF cells expressed stem/progenitor markers and were multipotent *in vitro,* which indicates *Scx* can label a subpopulation of AF progenitors. By constructing an IVD defect model, we found that treatment with *Scx*$^+$ cells promotes AF repair, demonstrating their therapeutic potential.

2. Results

Single-cell RNA sequencing analysis revealed that the transcription factor *Scx* specifically labels the cells of the outer annulus fibrosus.

To gain insight into the cellular and molecular characteristics of the intervertebral disc at the single cell resolution, we performed single-cell RNA sequencing (scRNA-seq) of the lumbar disc from 8-week wild-type mice. The total number of sequenced cells was 6,228, distributed as follows: 1965 in Cluster 0, 1531 in Cluster 1, 885 in Cluster 2, 424 in Cluster 3, 401 in Cluster 4, 375 in Cluster 5, 286 in Cluster 6, 168 in Cluster 7, 107 in Cluster 8, 54 in Cluster 9, and 32 in Cluster 10. Eleven distinct cell populations were identified, including: outer AF cells (proteoglycan 4, Prg4), inner AF cells (collagen type IX alpha 1, Col9a1), nucleus pulposus cells (keratin 8, Krt8), basophils (serine protease 34, Prss34), endothelial cells (protein tyrosine phosphatase receptor type B, Ptprb), red blood cells (carbonic anhydrase 1, Car1), Pre B cells (V-Set Pre-B cell surrogate light chain 1, Vpreb1), neutrophils (S100 calcium binding protein A8, S100a8), B cells (immunoglobulin Kappa constant, Lgkc), mononuclear macrophage cells (lymphocyte antigen 6C2, Ly6c2), and proliferating cells (proliferating cell nuclear antigen clamp associated factor, Pclaf) (Fig. 1A–C). To identify the stem/progenitor cell population of the annulus fibrosus, we performed pseudotime analysis, which revealed a trajectory from the outer annulus fibrosus cells to the inner annulus fibrosus cells, indicating that the stem/progenitor cells reside in the outer annulus fibrosus (Fig. 1D). We screened transcription factors highly expressed in the annulus fibrosus cell group, such as *Nfatc1, Hes1, Klf9* and *Csrnp*, as candidates for labeling stem/progenitor cells. However, most of these transcription factors were not only expressed in the annulus fibrosus but also widely distributed among other cell groups of the intervertebral disc (Fig. 1E). Interestingly, we found that *Scx* was specifically expressed in the outer annulus fibrosus (Fig. 1F). We used Monocle 2 unsupervised pseudotime to model the relationship between these two clusters, which revealed nine states (Figure below left). There are eight states (states 1–8) of outer AF cells linked to inner AF cell fate (state 9) (Fig. S1A). Interestingly, the majority of *Scx*$^+$ cells located in state 1 representing an early state among these cell populations (Fig. S1B). Further GO analysis of *Scx*$^+$ AF cells revealed that high expression of *Scx* was associated with extracellular structure organization, extracellular matrix organization, connective tissue maturation, and the transforming growth factor beta receptor signaling pathway (Fig. 1G).

2.1. Fate mapping revealed that Scx-lineage AF cells contribute to AF maturation

To study the function of *Scx*$^+$ AF cells during maturation, we constructed *Scx-CreER; Rosa26-Ai9* (*R26-Ai9*) mice. The *Scx-CreER; R26-Ai9* mice were induced by tamoxifen at post-natal day 1 (d1) and analyzed at d3 and 8 weeks(w8) (Fig. 2A). At d3, a few *Ai9*$^+$ cells were highly restricted to the outer AF, whereas by w8, Ai9$^+$ cells were distributed throughout most of the AF, demonstrating the massive expansion of *Scx*-lineage cells (Fig. 2A and B). To study the function of *Scx*$^+$ AF cells during homeostasis, the adult (8 weeks old) *Scx-CreER; R26-Ai9* mice were induced by tamoxifen and analyzed after 2 days and 8 weeks (Fig. 2C). Interestingly, the Ai9$^+$ cells did not show significant expansion (Fig. 2C and D). Most Ai9$^+$ cells expressed *ScxGFP* after consecutive tamoxifen induction (Fig. 2E). We then utilized a cell-proliferation tracing system named 'ProTracer' (Proliferation Tracer) to trace the proliferating cells within the AF. ProTracer (*R26-DreER; Ki67-CrexER; ScxGFP; R26-Ai9*) mice enable lifelong, noninvasive monitoring of cell proliferation following tamoxifen induction. Briefly, tamoxifen-induced *DreER-rox* recombination converts the inducible *Ki67-CrexER* into constitutively active *Ki67-Cre* in *DreER*-expressing cells, permanently recording active *Ki67* transcription by activating the *R26-Ai9* reporter (Fig. 2F) [18]. We induced ProTracer mice at d1 and 8 weeks of age with tamoxifen and analyzed them after 2 months. *Ki67*$^+$ cells were distributed throughout the AF following d1 induction, whereas their numbers decreased significantly with adult induction (Fig. 2G and H). These data demonstrate that *Scx*-lineage AF cells contribute to AF maturation.

2.2. Limited repair capacity of AF in adult mice

To study *Scx*-lineage cells during repair, we established a caudal vertebra puncture model in 8-week-old *Scx-CreER; ScxGFP; R26-Ai9* mice. After the tamoxifen induction, adult *Scx-CreER; ScxGFP; R26-Ai9* mice were treated with the caudal vertebra puncture and were analyzed at 4, 7, 14, and 28 days post-injury. Ai9$^+$ cells did not exhibit significant expansion, indicating limited damage repair capacity of the AF (Fig. 3A and B). EdU staining of the IVD at 4, 7, 14, and 28 days post-puncture revealed a significantly lower number of EdU$^+$ cells in the AF (Fig. 3C and D). The TUNEL staining of AF cells on the day 4, day 7, day 14 and day 28 after puncture showed that the number of TUNEL$^+$ cells in AF was significantly higher on day 4 and 7 than that on day 14 and 28, suggesting that a large number of cells would undergo apoptosis in the early stages of injury (Fig. 3E and F).

2.3. Clonogenicity and multipotency of Scx$^+$ progenitors

FACS analysis revealed that nearly all *Scx*$^+$ cells were negative for Lin markers (CD31/CD45/TER119) (Fig. 4A). Interestingly, Lin$^-$*Scx*$^+$ cells exhibited higher expression of stem/progenitor markers, including Sca1, CD200, CD73, Nestin, and CD44, compared to Lin$^-$*Scx*$^-$ cells (Fig. 4B).The colony formation assay of *Scx*$^-$ AF cell and *Scx*$^+$ AF cell from *ScxGFP* mice showed that Lin$^-$*ScxGFP*$^+$ cells had better capacity to form colonies compared with Lin$^-$*ScxGFP*$^-$ cells (Fig. 4C). Alcian blue staining also showed *Scx*$^+$ cells exhibited stronger chondrogenic differentiation than *Scx*$^-$ cells (Fig. 4D). After differentiation, Scx$^+$ cells showed higher transcriptional levels of chondrogenic markers, including *Aggrecan, Col2a1*, and *Sox9*, compared to *Scx*$^-$ cells (Fig. 4F). Alkaline phosphatase (ALP) and alizarin red S (ARS) staining revealed that *Scx*$^+$ cells exhibited stronger osteogenic differentiation than *Scx*$^-$ cells (Fig. 4E). After differentiation, *Scx*$^+$ cells displayed higher transcriptional levels of osteogenic markers, including *Alp, Bsp*, and *Opn*, compared to *Scx*$^-$ cells (Fig. 4F). However, *Scx*$^+$ cells exhibited weaker adipogenic differentiation than *Scx*$^-$ cells by Oil Red O staining (Fig. 4G). Taken together, these data indicated that *Scx* could label a subpopulation of AF progenitors.

2.4. Inhibition of the postnatal maturation of AF tissue by ablation of Scx$^+$ cells

During postnatal growth, the size and cell number of the AF increased significantly. To further verify the role of *Scx*$^+$ cells in the postnatal AF growth, we crossed *Scx-CreER; R26-Ai9* mice with *Rosa26-DTA (DTA)* mice. *Scx-CreER; R26-Ai9; DTA* mice and *Scx-CreER; R26-Ai9* (Control) received a dose of Tamoxifen (Tam) at d1 (Fig. 5A). IVD samples were harvested when the mice were 8 weeks old. *Ai9*$^+$ cells decreased, and the depletion of *Scx*$^+$ cells led to abnormal AF morphology (Fig. 5B and C). Both the size and cell numbers of the AF were reduced (Fig. 5D and E). Taken together, these data indicate that the expansion of *Scx*$^+$ progenitor cells is indispensable for the early postnatal maturation of AF.

2.5. Therapeutic potential of Scx$^+$ progenitors for AF healing

KEGG analysis of *Scx*$^+$ AF cells revealed that the *Scx* gene is

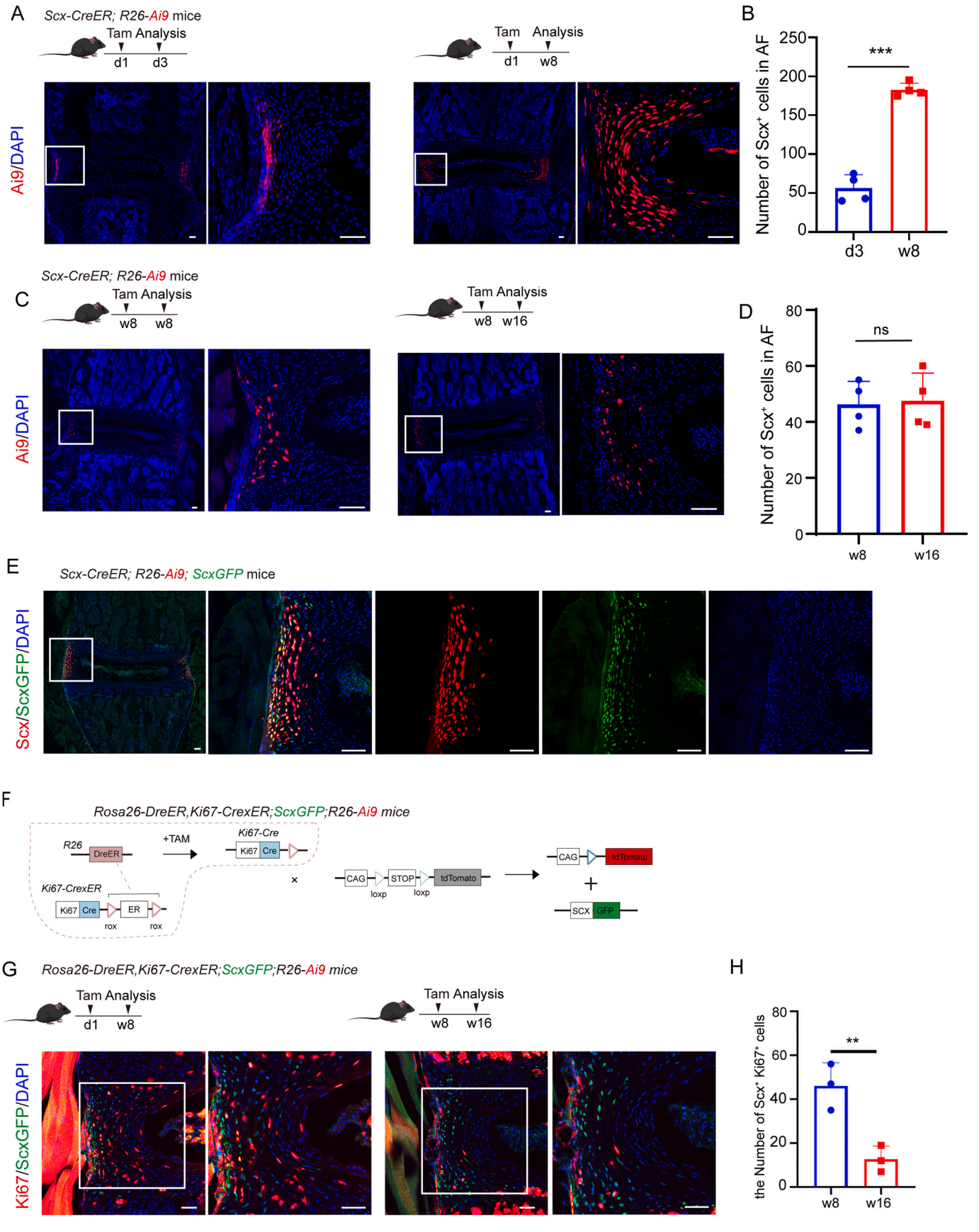

(caption on next page)

Fig. 2. Fate mapping showed that *Scx*-lineage AF cells contributed to the maturation of the AF
(A) Comparison of *Scx*$^+$ AF cells between mice induced by tamoxifen at day 1(d1) for one time and analyzed at d3 or 8 weeks (w8). n = 4 mice per group. (B) Quantitative analysis of the numbers of *Scx*$^+$ AF cells in (A). (C) Comparison of *Scx*$^+$ AF cells between mice induced by tamoxifen at 8 weeks for one time and analyzed after two days with mice induced by tamoxifen at 8 weeks and analyzed at 16 weeks. n = 4 mice per group. (D) Quantitative analysis of the numbers of *Scx*$^+$ AF cells in (C). (E) Confocal image showed the co-localization of *Scx-CreER*$^+$ cells and *ScxGFP*$^+$ cells. Mice were induced at 8 weeks old for five consecutive times and analyzed after 1 week. (F) The construction of Protracer mice. (G) Comparison of *Ki67*$^+$ AF cells between mice with different induction strategies. Mice were induced by tamoxifen at d1 or 8 weeks old for one time and analyzed after 8 weeks. n = 3 mice per group. (H) Quantitative analysis of the numbers of *Ki67*$^+$ AF cells in (G). Scale bars,100 μm. Data are presented as the mean ± SD. **,$p < 0.01$; ***,$p < 0.001$; ns,no significant difference, by unpaired, 2-tailed t test.

associated with PI3K-Akt signaling, Focal adhesion, ECM-receptor interaction and the TGF-β signaling pathway (Fig. 6A). The TGF-β signaling pathway has been reported to play a critical role in AF repair, but its effect on *Scx*$^+$ progenitor function remains unclear. Connective tissue growth factor (CTGF), a secreted protein involved in ECM remodeling during development and pathology, mediates the downstream actions of TGF-β [19]. We sorted and cultured the *Scx*$^+$ AF cells from the *Scx*GFP mice. *Scx*$^+$ AF cells displayed increased mRNA level of transcription factors (*Scx* and *Mkx*), ECM genes (*Col2a1, Aggrecan* and *Col1a1)* with the treatment of CTGF (Fig. 6B). *Scx*$^+$ progenitor cells are necessary to build the AF, express progenitor cell markers, and show multipotency and clonogenicity *in vitro*. We therefore explored the therapeutic potential of *Scx*$^+$ cells to enhance AF healing, with the long-term goal of developing a stem cell-based treatment for AF regeneration. *Scx*$^+$ cells were sorted, expanded *in vitro*, and transplanted into the injured AF. Different treatments were administered at the time of puncture. Analysis was performed 56 days after injury. SOFG staining revealed that, compared to the normal AF, the injured AF exhibited obvious defects and a disrupted structural boundary between the AF and the nucleus pulposus. Compared to the puncture group, AF treated with Matrigel alone showed no significant difference. Following injury, injection of Matrigel enclosing *Scx*$^-$ cells reduced the AF defect, but the structure between the nucleus pulposus and the AF remained disorganized. Compared to the Matrigel enclosing *Scx*$^-$ cells group, the AF structure in the Matrigel enclosing *Scx*$^+$ cells group was more regular. After injury, injection of Matrigel enclosing *Scx*$^+$ cells stimulated with CTGF resulted in a smaller AF defect and maintained the boundary between the AF and the nucleus pulposus (Fig. 6C). The average Modified Thompson Grading score was used to quantify AF structure. The results showed that compared with the normal annulus fibrosus, the scores in other groups were significantly higher. However, the score of the Matrigel enclosing *Scx*$^+$ cells stimulated by CTGF was relatively lower, while the area ratio of the inner AF to the total AF of the Matrigel enclosing *Scx*$^+$ cells stimulated by CTGF was significantly higher than that in the other puncture groups (Fig. 6D and E). The fluorescent images showed *ScxGFP*$^+$ cells resided in the AF region after transplantation and increased significantly with CTGF treatment, indicating that the transplanted cells could survive the transplantation and CTGF enhance the function of *Scx*$^+$ cells (Fig. S1C). These two results suggest that the treatment of the Matrigel enclosing *Scx*$^+$ cells stimulated by CTGF was more efficient.

3. Discussion

The adult IVD is normally non-regenerative since AF injury leads to decreased IVD cellularity, matrix degeneration, innervation, and inflammation [20]. Tissue regeneration utilizing resident progenitor cells may become a feasible strategy for IVD repair in the future. Sun et al. identified two new functional AF cell subpopulations with stemness and vascularization induction potential [21].

AF cells exposed to acute cyclic tensile strain showed significantly increased expression of the ECM gene Prg4.Prg4 is mechanically regulated in the AF [22]. Lubricin, the primary boundary lubricant for articular cartilage, protects against the development of osteoarthritis [23]. Shine et al. reported that lubricin, encoded by Prg4, is expressed in the AF of caprine IVDs [24]. Our study found that PRG4 is expressed in the outer AF of mice.

In addition to repair cells that deposit granulation tissue, immune cells such as pro-inflammatory macrophages, T lymphocytes, and mast cells have been implicated in poor adult AF healing [25–28]. However, mechanistic studies testing the requirement of these cells in healing have not been carried out and the sources of fibrotic repair cells remain largely unidentified. Our scRNA-seq results identified immune cell populations in the IVD, including basophils, Pre B cells, neutrophils, B cells, and mononuclear macrophage cells.

Adult annulocytes remained quiescent after injury, with minimal proliferation or cell recruitment observed overall. It is well known that the adult human IVD has limited capacity for endogenous repair and regeneration. This may result from a loss of proliferative capacity during maturation [29]. It has been reported that AF regeneration in neonatal mice depends on *Scx*-lineage cells, with neonatal mice capable of repair through the conversion of *Scx*-cells into *Scx*$^+$ cells [17]. This suggests that self-repair is not feasible in adulthood. *Scx*$^+$ cells can participate in repair in a IVD puncture model in neonatal mice but are unable to do so in adulthood [30]. However, AF injuries are most common in adults, so it is necessary to study treatment methods for AF injuries in adults. Our lineage tracing found that *Scx*$^+$ cells proliferated before 8 weeks of age. Injection of *Scx*$^+$ cells into the injury site of the adult AF has a reparative effect.

Transforming growth factor β3 (TGFβ3) is a potent anabolic growth factor and has been widely used for cartilage and tendon repair [31,32]. TGFβ3 plays an important role in promoting viability and ECM production [33–35]. The combined action of vanillin and TGFβ3 permitted the elimination of excess reactive oxygen substances (ROS), maintenance of the disc height, water content, the biomechanical property and promoted the regeneration of IVD [36]. Nanofibrous scaffold that releases basic fibroblast growth factor (bFGF) can promote AF repair and regeneration [37]. Connective tissue growth factor (CTGF), a secreted protein, can mediate several downstream actions of TGF-β [19]. CTGF plays a great role in angiogenesis and wound healing. CTGF significantly induced fibrogenic differentiation of BMSCs [38]. CTGF exhibits key properties beneficial to the healing process, including stimulating fibroblast proliferation and enhancing collagen deposition [39,40]. We found that CTGF can enhance the effect of *Scx* cells in repairing the AF.

Scx deficiency results in accelerated aging and imbalance of the Achilles tendon [41]. Some studies have shown that knockout of *Scx* during the embryonic stage does not affect the AF [42]. However, during the postnatal maturation stage, the depletion of *Scx*$^+$ cells may lead to abnormalities in the structure of the AF. We built *Scx-CreER; DTA* mice and found that ablating *Scx*$^+$ cells disturbed AF maturation.

It is worth mentioning that we chose an IVD injury model, which destroys almost all of the annulus fibrosus and probably affects the nucleus pulposus, in order to ensure that the degree of annular disruption was consistent in each experimental group. In this model, the AF was difficult to repair, but our cell transplantation efficiently repaired the AF.

Many studies are developing repair strategies to deliver cells or biomaterials to the IVD. However, cell delivery approaches have been particularly challenging due to the lack of a precise definition of AF cells and the absence of robust differentiation strategies [43]. AF repair strategies require considerations of safety, biocompatibility, and integration with native tissue [44]. Some studies indicated that adult cells of the AF derive from a population of *Scx*$^+$/*Sox9*$^+$ progenitors. This means that *Scx*$^+$ AF cells have differentiation ability and stem-progenitor cell

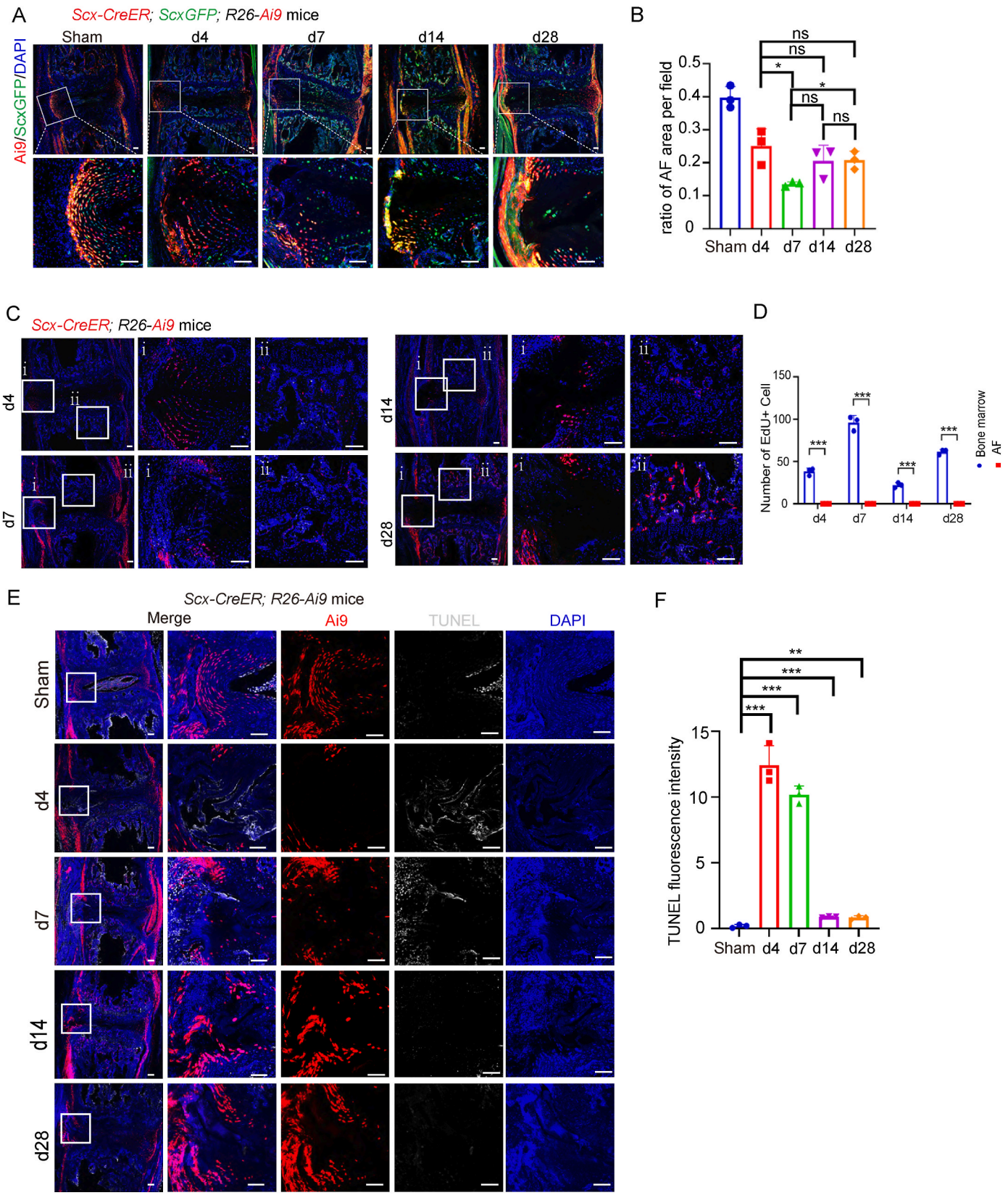

Fig. 3. Unrepairable AF in adult mice

(A)The caudal vertebra puncture model of 8-week-old *Scx-CreER; ScxGFP; R26-Ai9* mice on the 4th, 7th, 14th, and 28th days after puncture. n = 3 mice. (B) Quantitative analysis of the ratio of AF area to visual field area. (C) EdU staining of AF cells on the 4th, 7th, 14th and 28th day after puncture. n = 3 mice per group. (D) Quantitative analysis on the numbers of EdU^{+} AF cells in (C). (E) TUNEL staining of IVD on the 4th, 7th, 14th, and 28th days after puncture. n = 3 mice per group. (F) Quantitative analysis of the TUNEL fluorescence intensity in (E). *Scx-CreER; ScxGFP; R26-Ai9 or Scx-CreER; R26-Ai9* mice were induction by tamoxifen for 3–5 times continuously before injury. Data are presented as the mean ± SD. **,$p < 0.01$; ***,$p < 0.001$, by unpaired, 2-tailed t test.

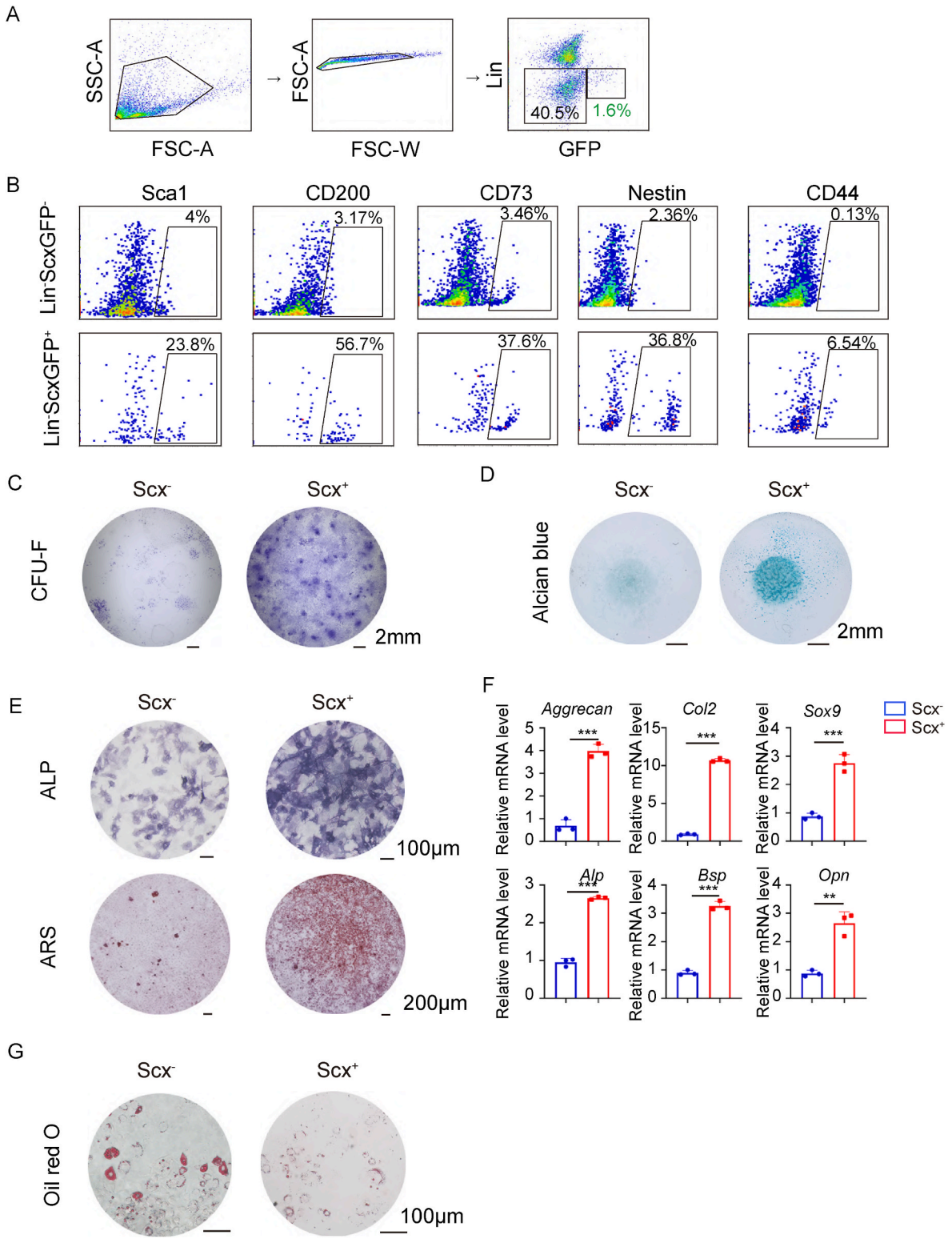

Fig. 4. Clonogenicity and multipotency of *Scx*$^+$ progenitors

(A) Flow cytometry analysis of Lin$^-$(CD45$^-$/Ter119$^-$/CD31$^-$) *ScxGFP*$^+$ cells. n = 5 mice. (B) The expression of Sca1, CD200, CD73, Nestin, and CD44 of Lin$^-$*Scx*GFP$^+$ and Lin$^-$*ScxGFP*$^-$ AF cells was assayed by FACS. n = 5 mice. (C) The colony formation assay of Lin$^-$*ScxGFP*$^+$ and Lin$^-$*ScxGFP*$^-$ AF cells by Crystal violet staining. Scale bars, 2 mm. (D) The Alcian blue staining of Lin$^-$*ScxGFP*$^+$ and Lin$^-$*ScxGFP*$^-$ AF cells after chondrogenic differentiation.Scale bars, 2 mm. (E) The ALP and ARS staining of Lin$^-$*ScxGFP*$^+$ and Lin$^-$*ScxGFP*$^-$ cells after osteogenic differentiation. Scale bars, 2 mm. (F) qPCR results showed that the mRNA levels of relative genes in Lin$^-$*ScxGFP*$^+$ and Lin$^-$*ScxGFP*$^-$ AF cells. Data are presented as the mean ± SD (n = 3). **,p < 0.01; ***,p < 0.001, by unpaired, 2-tailed t test. (G) The Oil Red O staining of Lin$^-$*ScxGFP*$^+$ and Lin$^-$*ScxGFP*$^-$ AF cells after adipogenic differentiation. Scale bars, 100 μm.

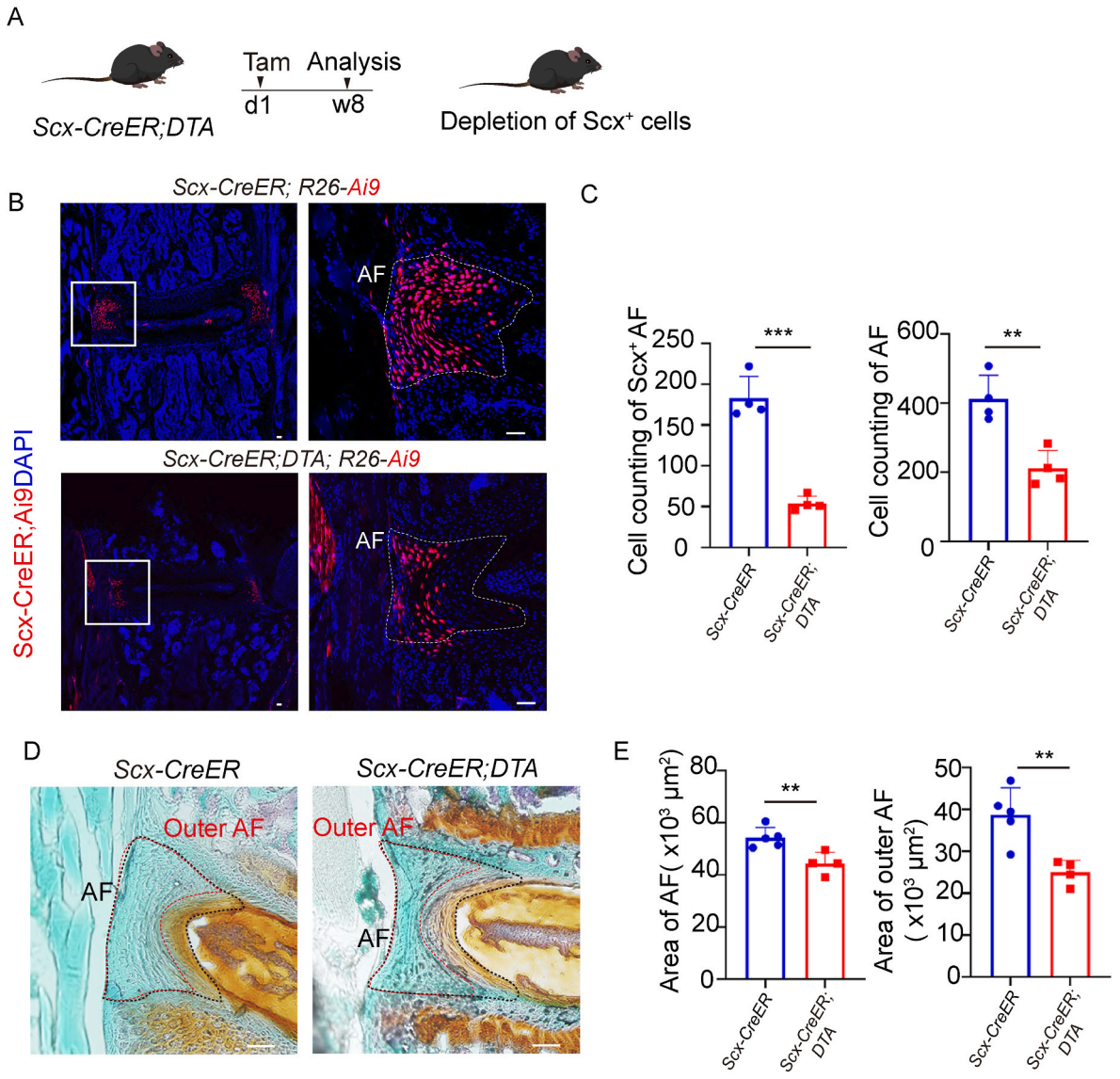

Fig. 5. Ablation of *Scx*$^{+}$ cells inhibits the postnatal maturation of AF tissue
(A) The strategy of ablating *Scx*$^{+}$ cells using *R26-DTA* mice. Mice were induced by intraperitoneal injection of tamoxifen (10 μl/g) for one time. (B) Representative confocal images of the cell number in the AF of control and *Scx-CreER; DTA* mice. n = 4 mice per group.Scale bars, 100 μm. (C) Quantitative analysis of AF cell number in (B). (D) SOFG staining showed the AF phenotype of Ctrl and *Scx-CreER; DTA* mice. n = 4 mice per group. Scale bars,100 μm. (E) Quantitative analysis of the area of AF. Data are presented as the mean ± SD. **,$p < 0.01$, by unpaired, 2-tailed t test.

characteristics [7]. Using *Scx* markers, we are able to refine the cell source for AF cell therapy to a certain extent. Currently, materials science is also focused on recruiting AF cells and promoting inflammatory repair through TGFβ [45]. Our research provides new basis for this (Fig. 7).

4. Methods

Animals. Scx-CreER mice were provided by Dr. Qiujian Zheng. *Rosa26-LSL-tdTomato (R26-Ai9)* mice were provided by *Dr. Zilong Qiu, and Rosa26-DTA (R26-DTA)* mice were provided by Dr. Aria Zeng. ProTracer mice were provided by Dr. Bin Zhou. ScxGFP mice were provided by Dr. Hongwei Ouyang. CreER-expressing mice were induced by intraperitoneal injection of tamoxifen (10 μl/g). Tamoxifen was dissolved in corn oil at a concentration of 10 mg/ml. We crossed *R26-DreER* mice, *Ki67-CrexER* mice, ScxGFP mice, and *R26-Ai9* mice to generate R*osa26-DreER; Ki67-CrexER; ScxGFP; R26-Ai9* mice [18]. We crossed *Scx-CreER; R26-Ai9* mice with ScxGFP mice to obtain *Scx-CreER; ScxGFP; R26-Ai9* mice. We crossed *Scx-CreER; R26-Ai9* mice with *Rosa26-DTA (DTA)* mice to generate *Scx-CreER; R26-Ai9; DTA* mice. All analyzed mice were maintained on the C57BL/6 background. Sex-matched littermate controls were used in all analyses. Both male and female mice were analyzed. All mice were bred and maintained under specific pathogen–free conditions.

Single-cell sequencing of sorted IVD cells from wild-type mice. Sorted cells obtained from the mouse IVD at 8 weeks were subjected to 10X Chromium Single Cell3′ Solution (version 2) library preparation according to the manufacturer's instructions (10X Genomics). Library sequencing was performed using an Illumina HiSeq 2500 sequencer, achieving a depth of 100 million reads per sample. Reads were converted to the fastq format using mkfastq in Cell Ranger 2.1.0 (10X Genomics). Reads were then aligned to the mouse reference genome (mm10, Ensembl annotation release 91). Alignment was performed using the count command of Cell Ranger 2.1.0 (10X Genomics). Primary analysis, quality control filtering (gene count per cell, unique molecular identifier counts per cell, and percentage of mitochondrial transcripts),

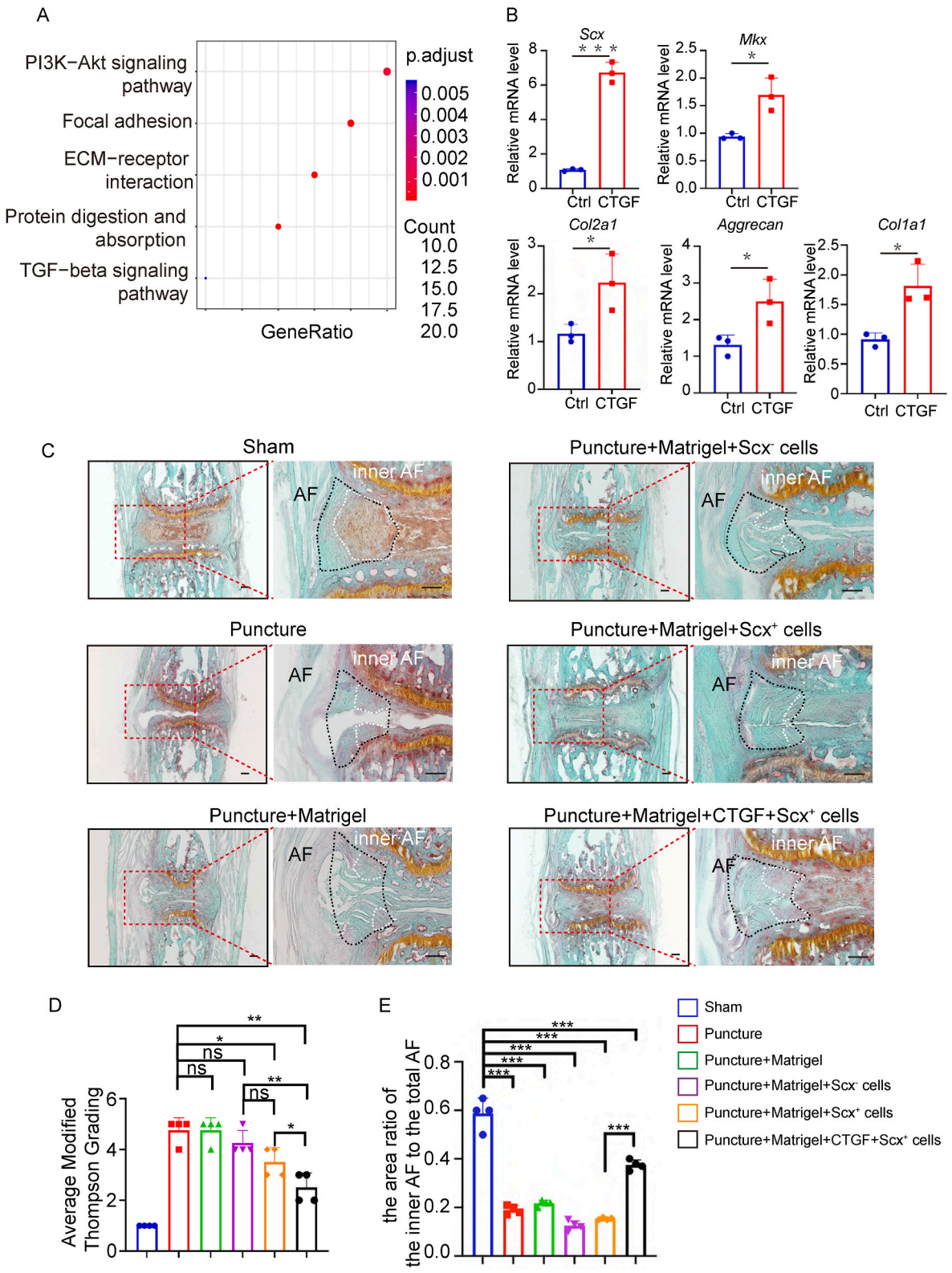

Fig. 6. Therapeutic potential of *Scx*$^{+}$ progenitors for AF healing

(A) KEGG analysis of *Scx*$^{+}$ cells from ScRNA-seq. (B) qPCR showed that the mRNA level of *Scx, Mkx, Col2a1, Aggrecan* and *Col1a1* in the *Scx*GFP $^{+}$ AF cells stimulated by CTGF and control. Data are presented as the mean ± SD (n = 3). $p < 0.05$; ***,p < 0.001, by unpaired, 2-tailed t test. (C) The SOFG staining of nude mice IVD puncture model with different treatments combined with Matrigel, with Lin^{-}*ScxGFP*$^{-}$ cells, with Lin^{-}*ScxGFP*$^{+}$cells with or without CTGF on the 56th day post-puncture. n = 4 mice per group. (D–E) Average Modified Thompson Grading of AF (D) and the area ratio of the inner AF to the total AF (n = 4) (E). Scale bars, 100 μm *, p < 0.05; **, p < 0.01; ***, p < 0.001, ns, no significant difference; as determined by ANOVA.

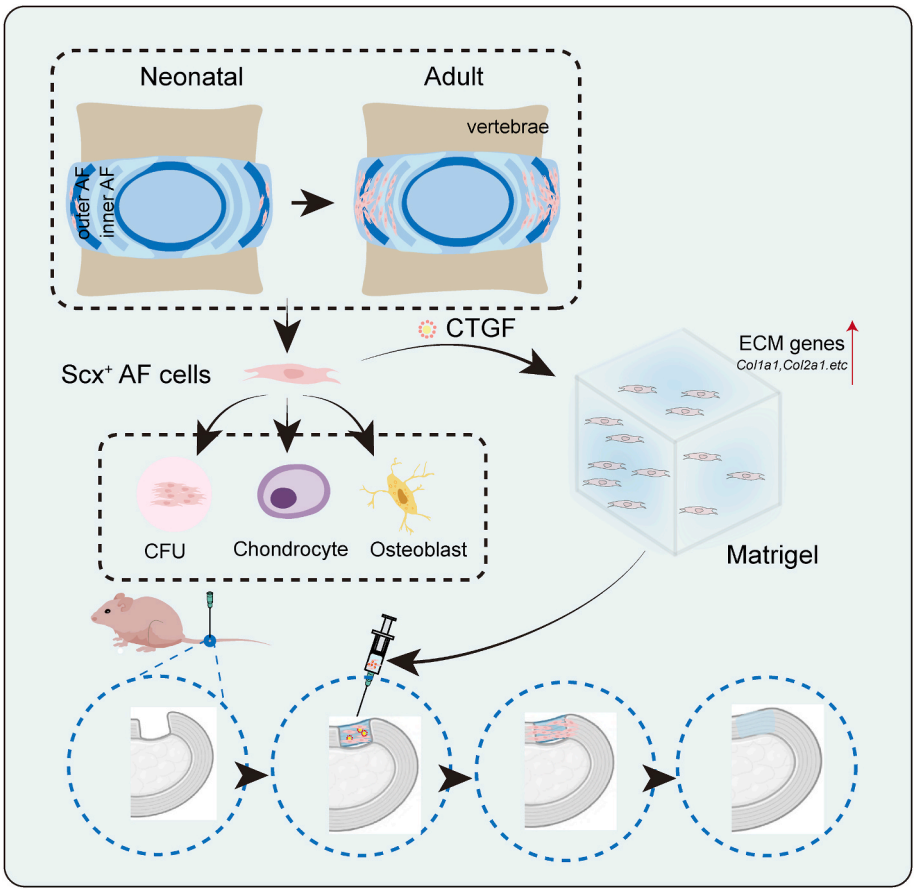

Fig. 7. Graphical Abstract
On the basis of single-cell RNA-sequencing (scRNA-seq) analysis of the intervertebral disc, we found that the transcription factor *Scleraxis* (*Scx*) can specifically label a progenitor cell population of the outer AF. By lineage tracing assay, *Scx*-lineage cells contribute to the maturation of the AF. The *Scx*-expressing AF cells are enriched for stem/progenitor cell markers and show a higher proliferative capacity and differentiation potential than the *Scx*⁻ cells. The ablation of *Scx*-expressing AF cells impairs the maturation of AF. Transplantation of *Scx*-lineage cells to injured AF with Connective tissue growth factor (CTGF) stimulation improved the AF healing.

clustering, cell-cycle phase scoring based on canonical markers and regression analysis, identification of cluster markers, and visualization of gene expression were performed using the Seurat (version 2.3) package for R. The Database for Annotation, Visualization and Integrated Discovery (DAVID) Functional Annotation Bioinformatics Microarray Analysis Test (https://david.ncifcrf.gov) was used for the Gene Ontology (GO) enrichment analysis of biological processes. Pseudotime Analysis: The single-cell trajectory analysis using Monocle 2 with DDR-Tree and default parameter was applied. Before Monocle analysis, marker genes of the Seurat clustering result and raw expression counts of the cells that passed filtering was selected. Based on the pseudotime analysis, branch expression analysis modeling was applied for the branch fate–determined gene analysis.

Histological analysis. For paraffin sections, spines were fixed in precooled 4 % paraformaldehyde (PFA) at 4 °C for 48 h, and decalcified in 10 % EDTA (pH 7.5). After PBS washing, the specimens were dehydrated in a graded ethanol series (70 %, 95 %, and 100 %), embedded in paraffin following xylene immersion, and sectioned at 7 μm thickness. The sections were stained with Hematoxylin-eosin staining(H&E)and Safranin O/fast green (SOFG) following standard procedures [46]. For frozen sections, the lumbar spine was fixed in precooled 4 % PFA at 4 °C for 48 h. After complete decalcification in 10 % EDTA, the samples were dehydrated in 30 % sucrose overnight, embedded in OCT compound (Tissue-Tek, 4583) and sectioned at 16–20 μm thickness using a Leica CM3050S freezing microtome. Nuclei were stained with DAPI (Millipore Sigma, D9542). Sections were mounted using fluorescence mounting medium (Dako, S3023). Imaging was performed with an Olympus FV3000 confocal microscope.

Isolation and culturing of AF cells. Primary AF cells were isolated from the lumbar IVDs of 4-week-old mice. After removing the nucleus pulposi, the annulus fibrosi were cut into pieces and digested with collagenase II (1.5 mg/mL; Millipore Sigma) and dispase II (2 mg/mL; Roche) for 30 min at 37 °C. The digestion solution was collected and centrifuged at 500g for 5 min. The isolated cells were cultured in a 6 cm dish containing α-MEM (Corning) supplemented with 10 % FBS.

FACS analysis. Cell sorting was performed using an Arial Sorp Cell Sorter (BD Biosciences). Adhesive cells and debris were excluded based on forward scatter (FSC) and side scatter (SSC) profiles.For the analysis of the *Scx*$^{+}$ cells from AF of *Scx*GFP mice, equal numbers of cells were aliquoted into individual tube containing different antibodies for immunostaining, following a previously described method. After removing RBCs from the AF-derived cells using RBC lysis buffer (Beyotime, C3702), the cells were stained with APC–anti–mouse CD24 (BioLegend, 138505), APC–anti–mouse Nestin (BioLegend, 655108), APC–anti-CD44 (BioLegend, 559250), APC–anti–mouse CD200 (BioLegend, 123809), PE/Cy7–anti–mouse CD105 (BioLegend, 120409), and APC–anti-Sca1 (eBioscience, 17-5981-81). After PBS washes, flow cytometric analysis was performed using Beckman CytoFlex FCM.

Colony formation assay and multipotent differentiation. For the colony formation assay, approximately 100 sorted *Scx*$^{+}$ and *Scx*$^{-}$ cells from the AF of the *Scx*GFP mice were cultured for 7 days.

For osteogenesis, approximately 2×10^4 cells were seeded per well in 96-well plates containing α-MEM (Corning) supplemented with 10 % FBS and 1 % penicillin/streptomycin (Thermo Fisher Scientific). After

12 h, the medium was replaced with osteogenic differentiation medium containing 50 μg/mL ascorbic acid (Millipore Sigma) and 1 mg/mL glycerophosphate (Millipore Sigma). The medium was changed every 2 days. Osteogenic differentiation was assessed after 7 days using alkaline phosphatase staining and after 21 days using alizarin red S staining.

For adipogenesis, approximately 2 × 104 cells were seeded per well in 96-well plates containing α-MEM (Corning) supplemented with 10 % FBS and 1 % penicillin/streptomycin (Thermo Fisher Scientific). After 12 h, the medium was replaced with the differentiation medium consisting of solution A and solution B. Solution A consisted of α-MEM with 10 % FBS, 50 mM dexamethasone (Millipore Sigma), 100 nM rosiglitazone (Millipore Sigma), 500 nM 3-isobutyl-1-methylxanthine (IBMX) (Millipore Sigma), 10 mg/mL insulin (Millipore Sigma), and 1 % penicillin/streptomycin (Millipore Sigma). Adipogenic differentiation was assessed after 7 days using 0.5 % Oil Red O staining (Millipore Sigma) and BODIPY (Invitrogen).

For chondrogenesis, cells were harvested and resuspended in α-MEM supplemented with 10 % FBS and 1 % penicillin/streptomycin. Droplets (15 μL) containing 2.5 × 105 cells were carefully placed in the center of each well of a 24-well plate. After cells adhered at 37 °C for 2–4 h, 500 μL of chondrogenic medium including 1 % insulin-transferrin-selenium solution (ITS, Millipore Sigma), 10 ng/mL TGF-β3 (Pepro Tech), 100 nM dexamethasone (Millipore Sigma), 40 μg/mL proline (Millipore Sigma), 50 μg/mL l-ascorbic acid 2-phosphate (Millipore Sigma), and 1 mM sodium pyruvate (Thermo Fisher Scientific) was added. The medium was changed every 2 days and cells were stained with Alcian blue on day 10.

*Real-time RT-PCR analysis.*Total RNA was *extracted* using TRIzol (Millipore Sigma) and reverse-transcribed into cDNA with the PrimeScript RT Reagent Kit (TaKaRa). Real-time quantitative PCR was performed *using* the Bio-Rad CFX96 system. The sequences of oligonucleotides used for quantitative PCR are listed in Supplemental Table 1.

Establishment of IVD Defect Model. Mice weighing 20–25 g and were 8–10 weeks old *were used for* surgery. A needle puncture-induced AF defect model was employed to determine the repair efficacy. According to different surgical procedures, mice were divided into two groups: (1) sham; (2) puncture. A longitudinal incision of approximately 2 cm in length was made *along* the midline posterior to the tail to expose the IVD, and then the IVD was punctured with a 25-gauge needle. This procedure created a full-thickness AF defect with a diameter of 0.60 mm. The wound was then sutured and disinfected.

Stimulation of Scx+ AF cells with CTGF. The sorted *Scx*$^{+}$ cells were derived from the AF of 4 weeks old ScxGFP mice. The Scx^{+} cells were expanded for 1 week and stimulated with 50 ng/ml CTGF for 48 h before transplantation.

Treatment of IVD injury model. After establishing the IVD Defect model in nude mice, the defect was injected with approximately 5 μL of Matrigel, either with or without 10,000 AF cells. *Scx*-negative and *Scx*-positive cells were isolated from the annulus fibrosus of *Scx-GFP* mice for use in injection experiments. According to different treatments, the nude mice were divided into six groups: (1) sham; (2) puncture; (3) puncture and injected with Matrigel; (4) puncture and injected with Matrigel and *Scx*$^{-}$cells; (5) puncture and injected with Matrigel and *Scx*$^{+}$ cells; (6) puncture and injected with Matrigel and *Scx*$^{+}$ cells stimulated by CTGF. After injection, the syringe was left in place for 5 min to allow the Matrigel to solidify, preventing leakage of Matrigel or cells and minimizing cell loss. After 4 weeks, samples were analyzed histologically.

Statistics. All results are expressed as the mean ± SEM. Comparisons between two groups were analyzed using two-tailed, unpaired Student's t test. For multiple-group comparisons, ANOVA followed by Tukey's post hoc test was used.

Study approval. All experiments were performed according to the protocol approved by the Animal Care and Use Committee of the Institute of Biochemistry and Cell Biology, Shanghai Institutes for Biological Sciences, Chinese Academy of Sciences.

Author contributions

H.J., S.D., W.Z. and H.F. conceived the study and designed the experiments. H.J. performed most of the research. J.W. and X.H. assisted with the mouse experiments. S.C. completed the analysis of single-cell RNA sequencing data. H.F. and H.J. analyzed data and wrote the paper. J.S., S.D., and W.Z. approved the manuscript.

Declaration of competing interest

The authors declare that they have no known competing financial interests or personal relationships that could have appeared to influence the work reported in this paper.

Acknowledgments

We thank the core facility for cell biology and the animal core facility of Shanghai Institute of Biochemistry and Cell Biology for assistance. This study was supported in part by grants from the National Natural Science Foundation of China (NSFC) [82472450, 82071809, 82102569] and the Strategic Priority Research Program of the Chinese Academy of Sciences, Grant No. XDB19000000, the China National Postdoctoral Program for Innovative Talents (BX2021309), and the Shanghai Postdoctoral Excellence Program (2021506).

Appendix A. Supplementary data

Supplementary data to this article can be found online at https://doi.org/10.1016/j.jot.2025.04.009.

References

[1] Diseases GBD, Injuries C. Global incidence, prevalence, years lived with disability (YLDs), disability-adjusted life-years (DALYs), and healthy life expectancy (HALE) for 371 diseases and injuries in 204 countries and territories and 811 subnational locations, 1990-2021: a systematic analysis for the Global Burden of Disease Study 2021. Lancet 2024;403:2133–61. https://doi.org/10.1016/S0140-6736(24)00757-8.

[2] Knezevic NN, Candido KD, Vlaeyen JWS, Van Zundert J, Cohen SP. Low back pain. Lancet 2021;398:78–92. https://doi.org/10.1016/S0140-6736(21)00733-9.

[3] Zhang Y, Xiong C, Kudelko M, Li Y, Wang C, Wong YL, et al. Early onset of disc degeneration in SM/J mice is associated with changes in ion transport systems and fibrotic events. Matrix Biol 2018;70:123–39. https://doi.org/10.1016/j.matbio.2018.03.024.

[4] Kepler CK, Ponnappan RK, Tannoury CA, Risbud MV, Anderson DG. The molecular basis of intervertebral disc degeneration. Spine J 2013;13:318–30. https://doi.org/10.1016/j.spinee.2012.12.003.

[5] Li J, Liu C, Guo Q, Yang H, Li B. Regional variations in the cellular, biochemical, and biomechanical characteristics of rabbit annulus fibrosus. PLoS One 2014;9:e91799. https://doi.org/10.1371/journal.pone.0091799.

[6] Ghazanfari S, Khademhosseini A, Smit TH. Mechanisms of lamellar collagen formation in connective tissues. Biomaterials 2016;97:74–84. https://doi.org/10.1016/j.biomaterials.2016.04.028.

[7] Sugimoto Y, Takimoto A, Akiyama H, Kist R, Scherer G, Nakamura T, et al. Scx+/Sox9+ progenitors contribute to the establishment of the junction between cartilage and tendon/ligament. Development 2013;140:2280–8. https://doi.org/10.1242/dev.096354.

[8] Best KT, Korcari A, Mora KE, Nichols AE, Muscat SN, Knapp E, et al. Scleraxis-lineage cell depletion improves tendon healing and disrupts adult tendon homeostasis. Elife 2021;10. https://doi.org/10.7554/eLife.62203.

[9] Feng H, Xing W, Han Y, Sun J, Kong M, Gao B, et al. Tendon-derived cathepsin K-expressing progenitor cells activate Hedgehog signaling to drive heterotopic ossification. J Clin Investig 2020;130:6354–65. https://doi.org/10.1172/JCI132518.

[10] Pryce BA, Brent AE, Murchison ND, Tabin CJ, Schweitzer R. Generation of transgenic tendon reporters, ScxGFP and ScxAP, using regulatory elements of the scleraxis gene. Dev Dyn 2007;236:1677–82. https://doi.org/10.1002/dvdy.21179.

[11] Torre OM, Mroz V, Bartelstein MK, Huang AH, Iatridis JC. Annulus fibrosus cell phenotypes in homeostasis and injury: implications for regenerative strategies. Ann N Y Acad Sci 2019;1442:61–78. https://doi.org/10.1111/nyas.13964.

[12] Wang J, Huang Y, Huang L, Shi K, Wang J, Zhu C, et al. Novel biomarkers of intervertebral disc cells and evidence of stem cells in the intervertebral disc. Osteoarthr Cartil 2021;29:389–401. https://doi.org/10.1016/j.joca.2020.12.005.

[13] Wang H, Wang D, Luo B, Wang D, Jia H, Peng P, et al. Decoding the annulus fibrosus cell atlas by scRNA-seq to develop an inducible composite hydrogel: a novel strategy for disc reconstruction. Bioact Mater 2022;14:350–63. https://doi.org/10.1016/j.bioactmat.2022.01.040.
[14] Liu C, Guo Q, Li J, Wang S, Wang Y, Li B, et al. Identification of rabbit annulus fibrosus-derived stem cells. PLoS One 2014;9:e108239. https://doi.org/10.1371/journal.pone.0108239.
[15] Jin L, Liu Q, Scott P, Zhang D, Shen F, Balian G, et al. Annulus fibrosus cell characteristics are a potential source of intervertebral disc pathogenesis. PLoS One 2014;9:e96519. https://doi.org/10.1371/journal.pone.0096519.
[16] Gruber HE, Riley FE, Hoelscher GL, Ingram JA, Bullock L, Hanley Jr EN. Human annulus progenitor cells: Analyses of this viable endogenous cell population. J Orthop Res 2016;34:1351–60. https://doi.org/10.1002/jor.23319.
[17] Torre OM, Mroz V, Benitez ARM, Huang AH, Iatridis JC. Neonatal annulus fibrosus regeneration occurs via recruitment and proliferation of Scleraxis-lineage cells. NPJ Regen Med 2019;4:23. https://doi.org/10.1038/s41536-019-0085-4.
[18] He L, Pu W, Liu X, Zhang Z, Han M, Li Y, et al. Proliferation tracing reveals regional hepatocyte generation in liver homeostasis and repair. Science 2021;371. https://doi.org/10.1126/science.abc4346.
[19] Tsai CC, Wu SB, Kau HC, Wei YH. Essential role of connective tissue growth factor (CTGF) in transforming growth factor-beta1 (TGF-beta1)-induced myofibroblast transdifferentiation from Graves' orbital fibroblasts. Sci Rep 2018;8:7276. https://doi.org/10.1038/s41598-018-25370-3.
[20] Iatridis JC, Michalek AJ, Purmessur D, Korecki CL. Localized intervertebral disc injury leads to organ level changes in structure, cellularity, and biosynthesis. Cell Mol Bioeng 2009;2:437–47. https://doi.org/10.1007/s12195-009-0072-8.
[21] Sun H, Wang H, Zhang W, Mao H, Li B. Single-cell RNA sequencing reveals resident progenitor and vascularization-associated cell subpopulations in rat annulus fibrosus. J Orthop Translat 2023;38:256–67. https://doi.org/10.1016/j.jot.2022.11.004.
[22] Kim MKM, Burns MJ, Serjeant ME, Seguin CA. The mechano-response of murine annulus fibrosus cells to cyclic tensile strain is frequency dependent. JOR Spine 2020;3:e21114. https://doi.org/10.1002/jsp2.1114.
[23] Ruan MZ, Erez A, Guse K, Dawson B, Bertin T, Chen Y, et al. Proteoglycan 4 expression protects against the development of osteoarthritis. Sci Transl Med 2013;5:176ra34. https://doi.org/10.1126/scitranslmed.3005409.
[24] Shine KM, Spector M. The presence and distribution of lubricin in the caprine intervertebral disc. J Orthop Res 2008;26:1398–406. https://doi.org/10.1002/jor.20614.
[25] Nerlich AG, Weiler C, Zipperer J, Narozny M, Boos N. Immunolocalization of phagocytic cells in normal and degenerated intervertebral discs. Spine (Phila Pa 1976) 2002;27:2484–90. https://doi.org/10.1097/00007632-200211150-00012.
[26] Nakazawa KR, Walter BA, Laudier DM, Krishnamoorthy D, Mosley GE, Spiller KL, et al. Accumulation and localization of macrophage phenotypes with human intervertebral disc degeneration. Spine J 2018;18:343–56. https://doi.org/10.1016/j.spinee.2017.09.018.
[27] Wiet MG, Piscioneri A, Khan SN, Ballinger MN, Hoyland JA, Purmessur D. Mast Cell-Intervertebral disc cell interactions regulate inflammation, catabolism and angiogenesis in Discogenic Back Pain. Sci Rep 2017;7:12492. https://doi.org/10.1038/s41598-017-12666-z.
[28] Shamji MF, Guha D, Paul D, Shcharinsky A. Systemic inflammatory and Th17 immune activation among patients treated for lumbar radiculopathy exceeds that of patients treated for persistent postoperative neuropathic pain. Neurosurgery 2017;81:537–44. https://doi.org/10.1093/neuros/nyx052.
[29] Dahia CL, Mahoney EJ, Durrani AA, Wylie C. Postnatal growth, differentiation, and aging of the mouse intervertebral disc. Spine (Phila Pa 1976) 2009;34:447–55. https://doi.org/10.1097/BRS.0b013e3181990c64.
[30] Torre OM, Das R, Berenblum RE, Huang AH, Iatridis JC. Neonatal mouse intervertebral discs heal with restored function following herniation injury. FASEB J 2018;32:4753–62. https://doi.org/10.1096/fj.201701492R.
[31] Peng Y, Li J, Lin H, Tian S, Liu S, Pu F, et al. Endogenous repair theory enriches construction strategies for orthopaedic biomaterials: a narrative review. Biomater Transl 2021;2:343–60. https://doi.org/10.12336/biomatertransl.2021.04.008.
[32] Bello AB, Kim Y, Park S, Muttigi MS, Kim J, Park H, et al. Matrilin3/TGFbeta3 gelatin microparticles promote chondrogenesis, prevent hypertrophy, and induce paracrine release in MSC spheroid for disc regeneration. NPJ Regen Med 2021;6:50. https://doi.org/10.1038/s41536-021-00160-0.
[33] Risbud MV, Di Martino A, Guttapalli A, Seghatoleslami R, Denaro V, Vaccaro AR, et al. Toward an optimum system for intervertebral disc organ culture: TGF-beta 3 enhances nucleus pulposus and anulus fibrosus survival and function through modulation of TGF-beta-R expression and ERK signaling. Spine (Phila Pa 1976) 2006;31:884–90. https://doi.org/10.1097/01.brs.0000209335.57767.b5.
[34] Chen S, Liu S, Ma K, Zhao L, Lin H, Shao Z. TGF-beta signaling in intervertebral disc health and disease. Osteoarthr Cartil 2019;27:1109–17. https://doi.org/10.1016/j.joca.2019.05.005.
[35] Hodgkinson T, Shen B, Diwan A, Hoyland JA, Richardson SM. Therapeutic potential of growth differentiation factors in the treatment of degenerative disc diseases. JOR Spine 2019;2:e1045. https://doi.org/10.1002/jsp2.1045.
[36] Zhu Z, Yu Q, Li H, Han F, Guo Q, Sun H, et al. Vanillin-based functionalization strategy to construct multifunctional microspheres for treating inflammation and regenerating intervertebral disc. Bioact Mater 2023;28:167–82. https://doi.org/10.1016/j.bioactmat.2023.05.005.
[37] Tu Z, Han F, Zhu Z, Yu Q, Liu C, Bao Y, et al. Sustained release of basic fibroblast growth factor in micro/nanofibrous scaffolds promotes annulus fibrosus regeneration. Acta Biomater 2023;166:241–53. https://doi.org/10.1016/j.actbio.2023.05.034.
[38] Wang L, Wei X, Duan C, Yang J, Xiao S, Liu H, et al. Bone marrow mesenchymal stem cell sheets with high expression of hBD3 and CTGF promote periodontal regeneration. Biomater Adv 2022;133:112657. https://doi.org/10.1016/j.msec.2022.112657.
[39] Liu YC, Chen SH, Kuan CH, Chen SH, Huang WY, Chen HX, et al. Assembly of interfacial polyelectrolyte complexation fibers with mineralization gradient for physiologically-inspired ligament regeneration. Adv Mater 2024;36:e2314294. https://doi.org/10.1002/adma.202314294.
[40] Shen H, Jayaram R, Yoneda S, Linderman SW, Sakiyama-Elbert SE, Xia Y, et al. The effect of adipose-derived stem cell sheets and CTGF on early flexor tendon healing in a canine model. Sci Rep 2018;8:11078. https://doi.org/10.1038/s41598-018-29474-8.
[41] Korcari A, Nichols AEC, Buckley MR, Loiselle AE. Scleraxis-lineage cells are required for tendon homeostasis and their depletion induces an accelerated extracellular matrix aging phenotype. Elife 2023;12. https://doi.org/10.7554/eLife.84194.
[42] Murchison ND, Price BA, Conner DA, Keene DR, Olson EN, Tabin CJ, et al. Regulation of tendon differentiation by scleraxis distinguishes force-transmitting tendons from muscle-anchoring tendons. Development 2007;134:2697–708. https://doi.org/10.1242/dev.001933.
[43] Guterl CC, See EY, Blanquer SB, Pandit A, Ferguson SJ, Benneker LM, et al. Challenges and strategies in the repair of ruptured annulus fibrosus. Eur Cell Mater 2013;25:1–21. https://doi.org/10.22203/ecm.v025a01.
[44] Long RG, Torre OM, Hom WW, Assael DJ, Iatridis JC. Design requirements for annulus fibrosus repair: review of forces, displacements, and material properties of the intervertebral disk and a summary of candidate hydrogels for repair. J Biomech Eng 2016;138:021007. https://doi.org/10.1115/1.4032353.
[45] Han F, Tu Z, Zhu Z, Liu D, Meng Q, Yu Q, et al. Targeting endogenous reactive oxygen species removal and regulating regenerative microenvironment at annulus fibrosus defects promote tissue repair. ACS Nano 2023;17:7645–61. https://doi.org/10.1021/acsnano.3c00093.
[46] Niu N, Xiang JF, Yang Q, Wang L, Wei Z, Chen LL, et al. RNA-binding protein SAMD4 regulates skeleton development through translational inhibition of Mig6 expression. Cell Discov 2017;3:16050. https://doi.org/10.1038/celldisc.2016.50.